Electronic Supplementary Material (ESI) for Analyst.

Supplementary Information

Flexible virtual sensor array based on laser-induced graphene and MXene for detecting volatile organic compounds in human breath

Dongsheng Li[a], Yuzhou Shao[b], Qian Zhang[a], Mengjiao Qu[a], Jianfeng Ping[b], Yong Qing Fu[c], Jin Xie[a,*]

[a] State Key Laboratory of Fluid Power and Mechatronic Systems, Zhejiang University, Hangzhou, Zhejiang 310027, China

[b] Laboratory of Agricultural Information Intelligent Sensing, School of Biosystems Engineering and Food Science, Zhejiang University, Hangzhou, Zhejiang 310058, China

[c] Faculty of Engineering and Environment, University of Northumbria, Newcastle upon Tyne NE1 8ST, UK

Corresponding author: Jin Xie

Email: xiejin@zju.edu.cn

Telephone Number: +86-15925641742

S1 Detailed synthesis processes of $Ti_3C_2T_x$

$Ti_3C_2T_x$ was synthesized by selective etching of Al from Ti_3AlC_2. Lithium fluoride (LiF) of 2 g and hydrochloric acid (HCl, 9 M and 40 ml) were stirred in a Teflon beaker for 30 min (400 rpm; IKA HS4). Ti_3AlC_2 (2 g) was slowly added into the above mixture, which was further stirred for 24 h at 35 °C. Then the mixture was centrifuged at 3500 rpm for 10 min. The obtained precipitates were diluted with deionized water and the formed dispersion was sonicated (750 W) for 10 min. The above steps were repeated until the pH value of the supernatant was above 5. Ethanol was added in the formed precipitate. The dispersion was sonicated for 1 h and centrifuged at 10000 rpm for 10 min. Deionized water was added in the resulting precipitate and the dispersion was sonicated for 20 min. After centrifugal process, the obtained black supernatant was collected.

S2 Material Characterizations Methods.

Raman spectrum was obtained using a laser confocal Raman microscopy (LabRAM HR Evolution, Horiba Jobin Yvon), in order to confirm the graphene formation by the laser induction process. A field emission scanning electron microscope (FE-SEM; SU-8100, Hitachi) equipped with an energy dispersive X-Ray spectrometer (EDS; X-max80, Oxford) was used to study the surface morphology and elements of the obtained flexible LIG-IDE and VOC sensor. An X-ray diffractometer (MAXima XRD-7000, Shimadzu) was used for X-ray diffraction (XRD) analysis. X-ray photoelectron spectroscopy (XPS, Escalab 250Xi, Thermo Fisher) was used to characterize the chemical components and chemical bonding structures of the $Ti_3C_2T_x$ film. XPS analysis was conducted through curve fitting and calculations using a Gaussian−Lorentzian method.

S3 Data Analysis Method.

Three sensors were tested under same conditions, and results were expressed using the mean value ± its standard deviation. Reactance is the defined as the imaginary part of impedance. VOC identification and concentration estimation models were built using eight representative parameters from the broadband impedance spectra of the VSA, i.e., the resistance values at 100 kHz, 5 MHz, 15 MHz and the reactance values at 300 kHz, 1 MHz, 3 MHz, 9 MHz, 20 MHz. Firstly, principal component analysis (PCA) was applied as an unsupervised pattern recognition tool for qualitative classification of multivariate data and to reduce the dimensionality of the original data set. PCA is a powerful machine learning tool that basically projects the data points into a new coordinate system, whose coordinates account for the largest variance in the original data [1]. Then the linear discrimination analysis (LDA) was performed as a supervised pattern recognition to quantitatively identify different test analytes [2]. The resultant principal components (PCs) in the PCA were used as the input variables to the LDA. Leave-one-out cross validation (LOOCV) was used as a cross-validation method to estimate the identification [2]. We applied a partial least square (PLS) regression with four latent variables (LVs) to quantify concentrations of ethanol vapor in a mixture. PLS regression determines the correlation between the independent variable (concentration of target VOC) and the sensor's response by finding the direction that explains the maximum variance of the independent variable in the multi-dimensional space of the VSA response [3]. Multivariate data processing (PCA, LDA and PLS) was performed in MATLAB programs in this work.

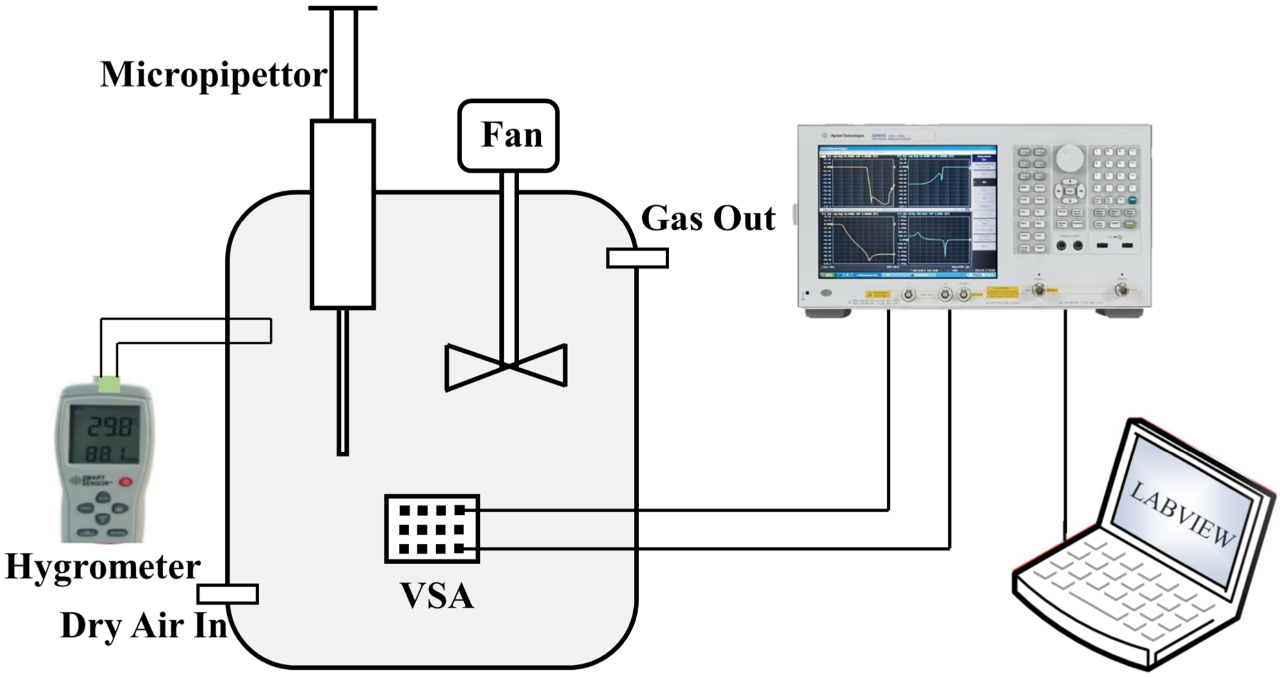

Figure S1. Schematic illustration of the VOC sensing system.

The desired VOC concentration was obtained by injecting the required quantity of anhydrous liquid analytes into a sealed glass container using a microliter syringe. The concentrations of targeted VOCs in the chamber were calculated using the following equation [4, 5]:

$$C = \frac{22.4\rho T V_s}{273MV} \times 1000 \qquad (1)$$

where *C* is the concentration of the gaseous VOC at the room temperature (ppm), ρ is the density of anhydrous liquid VOC ($g{\cdot}mL^{-1}$), *T* is the testing temperature (K), *Vs* is the volume of anhydrous liquid VOC (μL), *M* is the molecular weight of a VOC ($g{\cdot}mol^{-1}$), and *V* is the volume of the glass container (*L*) filled with the VOC. In this work, taking the ethanol as an example, the values of *M*, ρ and *T* are 46 $g{\cdot}mol^{-1}$, 0.789 $g{\cdot}mL^{-1}$ and 298 K, respectively. Dry air was supplied from an air cylinder and the container was cleaned by dry air flow at room temperature before doing each gas sensing test.

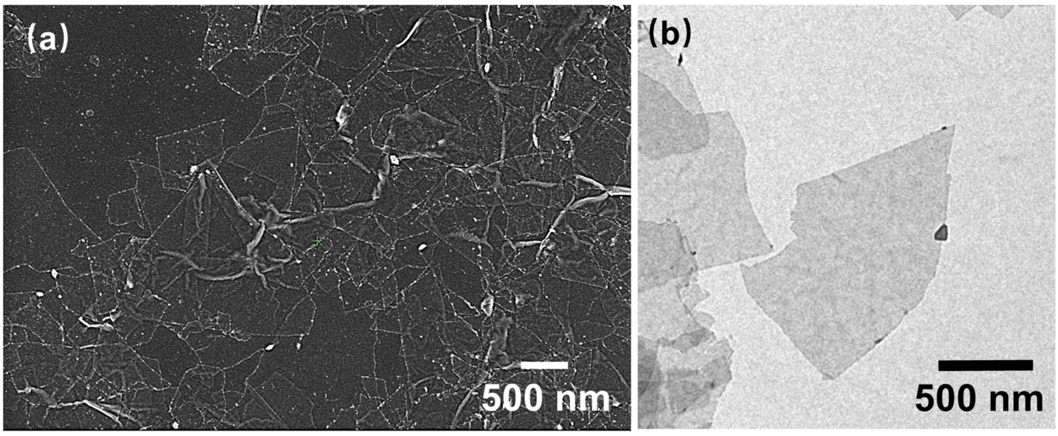

Figure S2. SEM (a) and TEM (b) images of $Ti_3C_2T_x$ nanosheets.

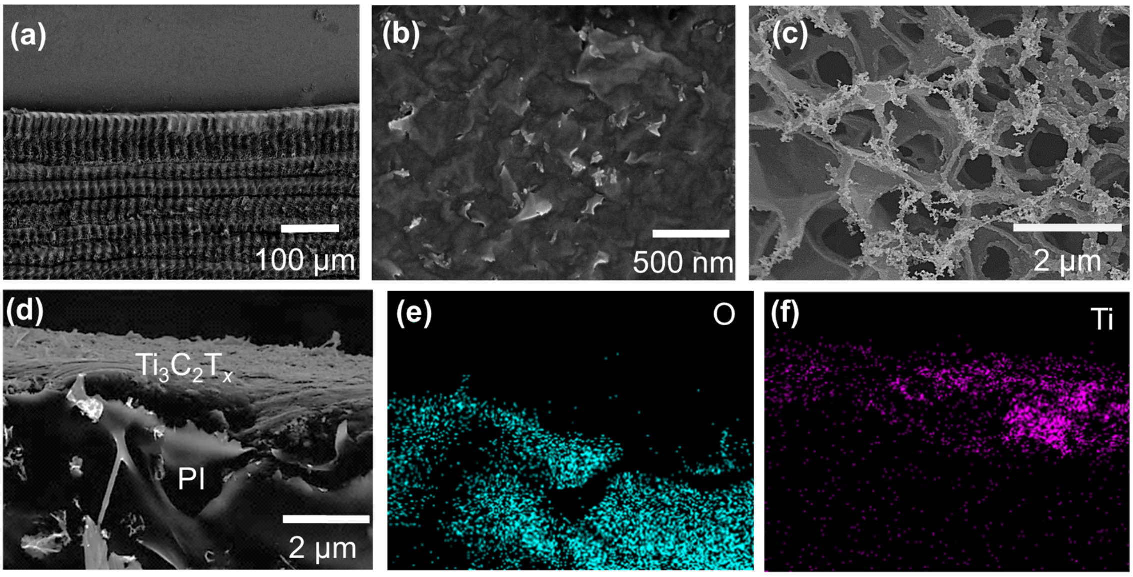

Figure S3. SEM images of the proposed sensor with $Ti_3C_2T_x$ film. (a) SEM image of the proposed sensor. (b) SEM image of $Ti_3C_2T_x$ film in the channel. (c) Surface SEM image of LIG-IDE after coating. Cross-sectional SEM image of the flexible sensor (in the channel) (d) and its corresponding elemental mapping analyses (O and Ti) (e, f).

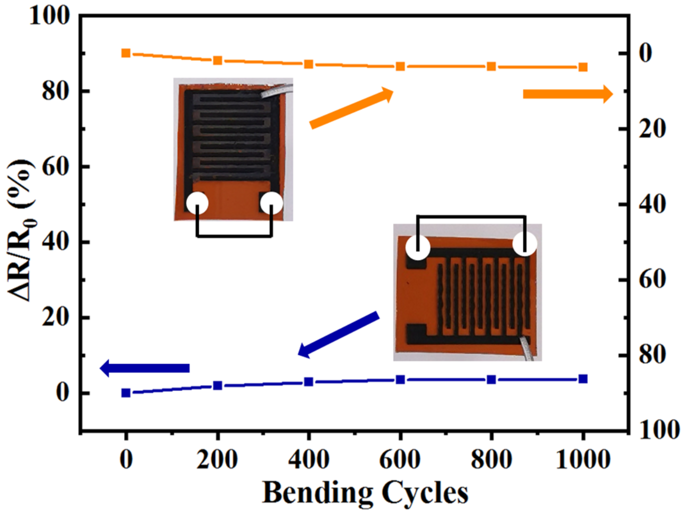

Figure S4. Changes in resistance of the flexible VOC sensor and LIG-IDE as a function of bending cycles.

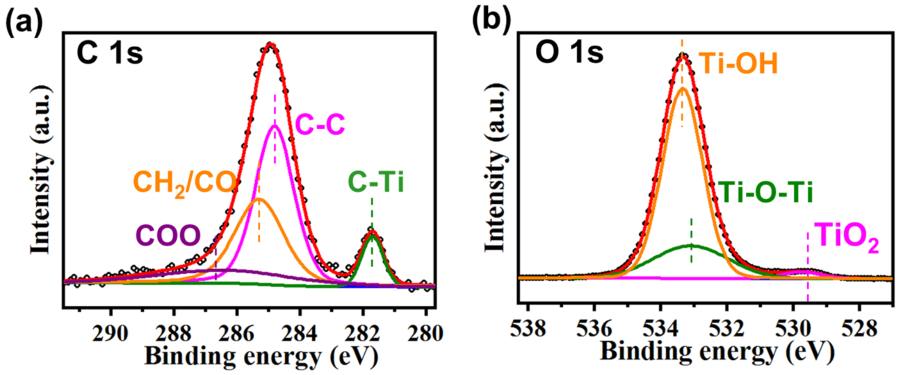

Figure S5. XPS of $Ti_3C_2T_x$ film at two core levels: (a) C 1s, (b) O 1s.

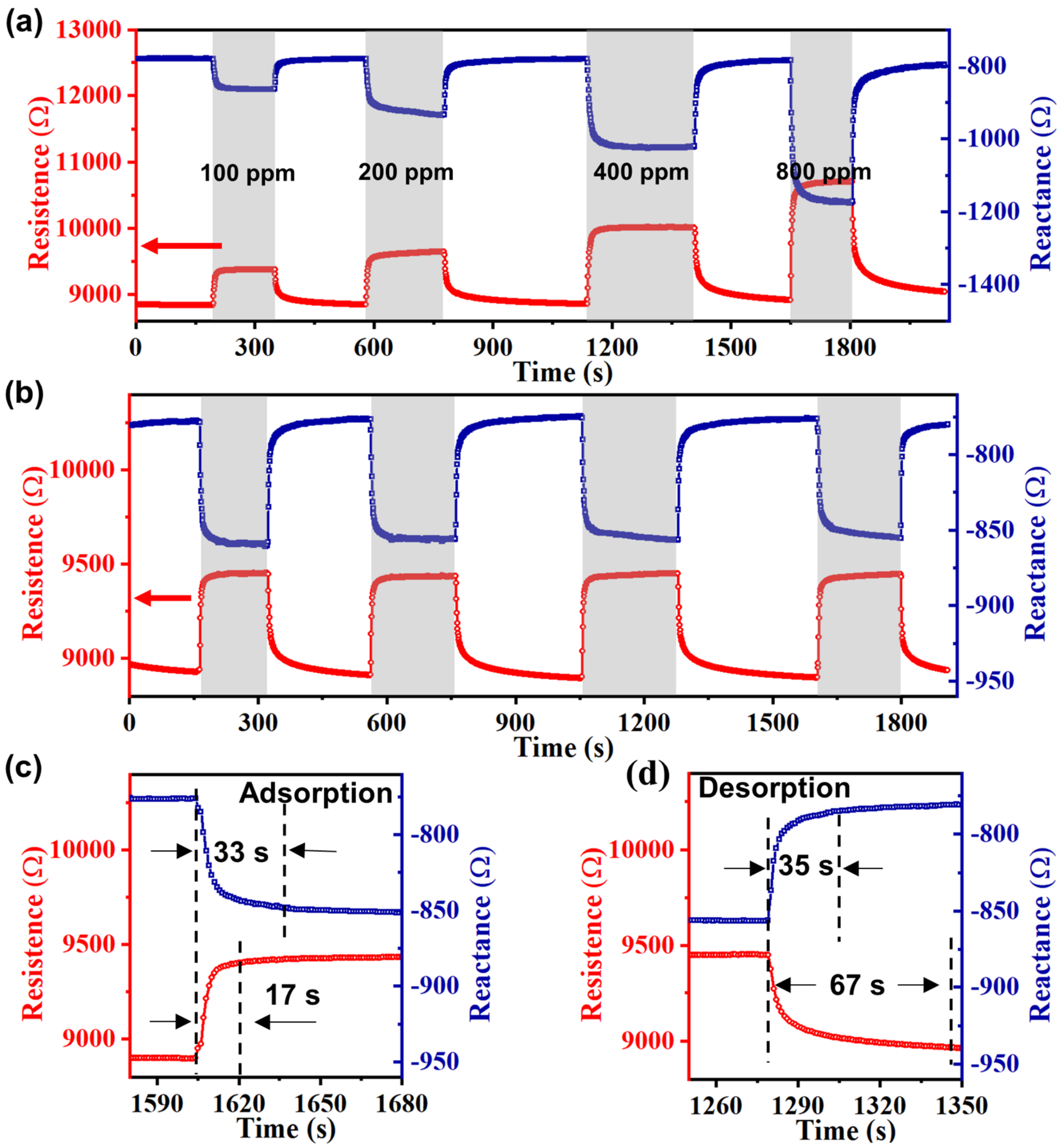

Figure S6. Dynamic response test of the $Ti_3C_2T_x$ based VOC sensor. (a) Continuous response of the resistance and reactance of the sensor operated at 1 MHz to different ethanol concentrations. (b) Short-term repeatability of sensor when the ethanol concentration is repeatedly changed. Detailed response (c) and recovery (d) processes of the sensor.

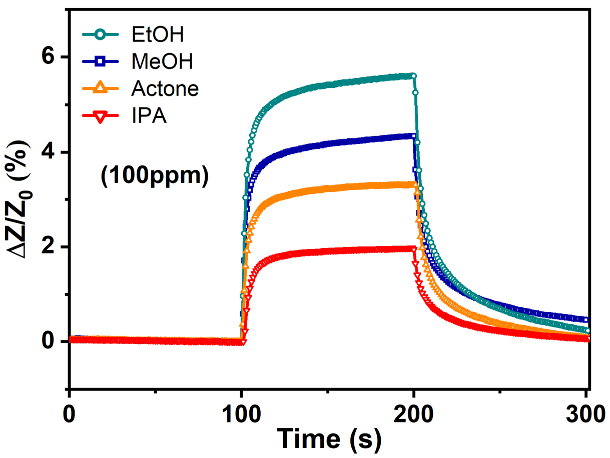

Figure S7. Impedance responses of the flexible sensor operated at 1 MHz to 100 ppm of 4 VOCs.

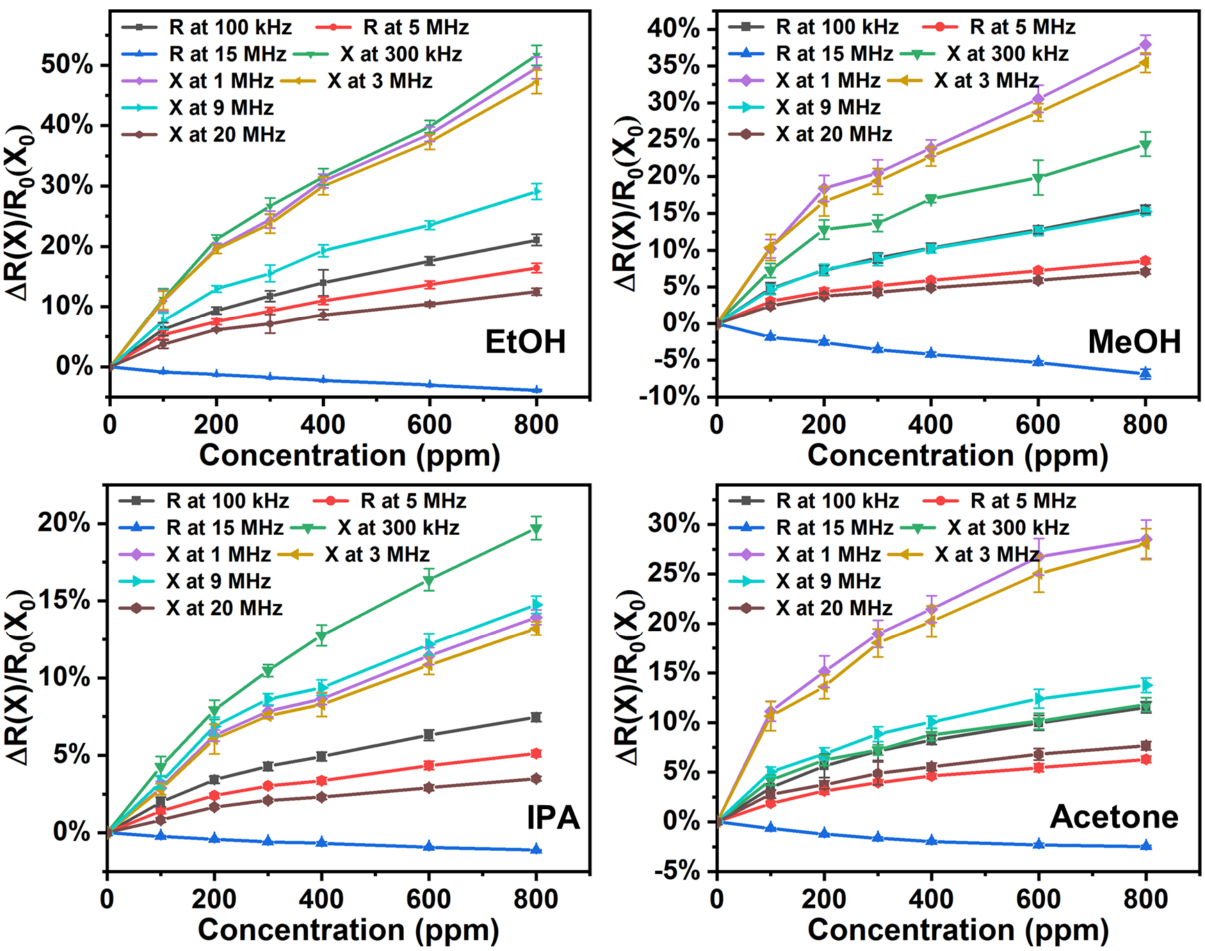

Figure S8. Unique fingerprint patterns of different VOCs.

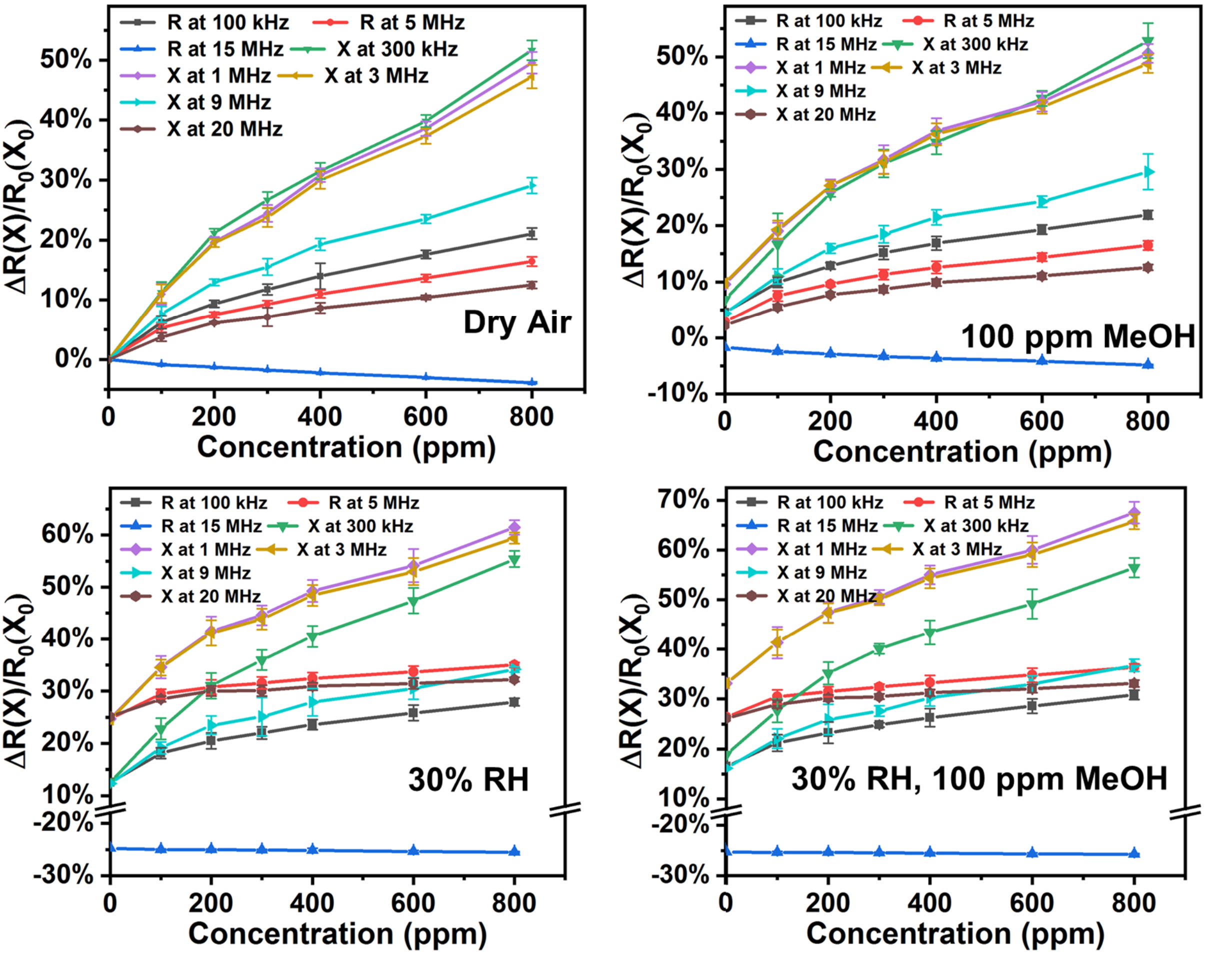

Figure S9. Responses of the sensor to ethanol in a background of variable humidity levels and methanol concentrations.

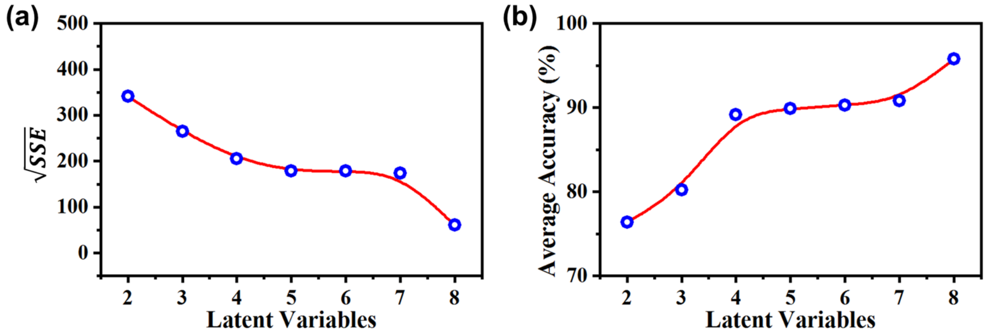

Figure S10. The root of SSE (a) and average accuracy (b) for prediction of ethanol concentration vary with the number of LVs.

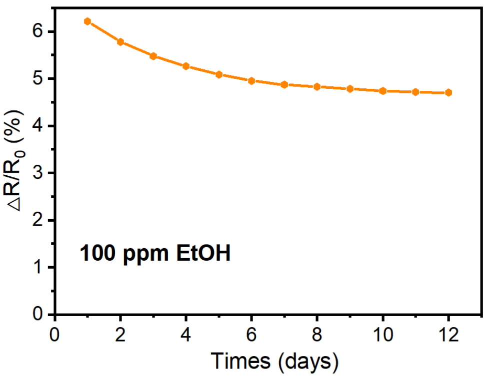

Figure S11. Stability of the MXene-based flexible VOCs sensor.

Table S1. The concentrations of mixtures.

A		B		C		D	
EtOH (ppm)	MeOH (ppm)	EtOH (ppm)	IPA (ppm)	EtOH (ppm)	Actone (ppm)	EtOH (ppm)	dichloromethane (ppm)
100	100	100	100	100	100	100	100
100	500	100	500	100	500	100	500
100	1000	100	1000	100	1000	100	1000
500	1000	500	1000	500	1000	500	1000
1000	1000	1000	1000	1000	1000	1000	1000

Reference

[1] Zhao, Y.; Yang, Q.; Chang, Y.; Qu, H.; Pang, W.; Zhang, H.; Duan, X. Detection and discrimination of volatile organic compounds using a single multi-resonance mode piezotransduced silicon bulk acoustic wave resonator (PSBAR) as virtual sensor array. Sens. Actuators, B 2018, 254, 1191-1199.

[2] Bur, C.; Bastuck, M.; Puglisi, D.; Schütze, A.; Lloyd Spetz, A.; Andersson, M. Discrimination and quantification of volatile organic compounds in the ppb-range with gas sensitive SiC-FETs using multivariate statistics. Sens. Actuators, B 2015, 214, 225-233.

[3] Potyrailo, R. A.; Bonam, R. K.; Hartley, J. G.; Starkey, T. A.; Vukusic, P.; Vasudev, M.; Bunning, T.; Naik, R. R.; Tang, Z.; Palacios, M. A.; Larsen, M.; Le Tarte, L. A.; Grande, J. C.; Zhong, S.; Deng, T. Towards outperforming conventional sensor arrays with fabricated individual photonic vapour sensors inspired by Morpho butterflies. Nat. Commun. 2015, 6, 7959: 1-12.

[4] Li, X.; Chang, Y.; Long, Y. Influence of Sn doping on ZnO sensing properties for ethanol and acetone. Mater. Sci. Eng. C 2012, 32 (4), 817-821.

[5] Ding, B.; Wang, X.; Yu, J.; Wang, M. Polyamide 6 composite nano-fiber/net functionalized by polyethyleneimine on quartz crystal microbalance for highly sensitive formaldehyde sensors. J. Mater. Chem. 2011, 21 (34), 12784.